ASPS Conference Proceedings 1: 891-900 (2022)

Proceedings of

12th Structural Engineering Convention-An International Event (SEC 2022)

Available at https://asps-journals.com/index.php/acp

Numerical Modelling of an Exterior RC Beam Column Joint Subjected to Cyclic Loading Strengthened Using UHPFRC and CFRP

Q. Fayaz [1,*], G. Kaur[2], P.P. Bansal[3]

[1] Department of Civil Engineering, M.E. Structures, TIET, Patiala, 147001, India
[2] Department of Civil Engineering, Assistant Professor, TIET, Patiala, 147001, India
[3] Department of Civil Engineering, Associate Professor and Head of Department, TIET, Patiala, 147001, India

Paper ID - 060436

Abstract

A poorly detailed reinforced concrete (RC) beam-column joint (BCJ) is highly susceptible to damage under seismic forces due to the generation of shear stresses. Shear stresses are generated due to the continuous change in the direction of the compression and tension forces acting on the beam-column joint. As a result, the strength, stiffness and the energy dissipation of the whole structure is affected. It needs to be addressed beforehand by improving its shear, tensile and energy dissipation capacities so that the damage is minimised. So a structure needs to be strengthened prior to any major damage. In the present study the seismic performance assessment of a BCJ strengthened by a combination of ultra-high performance fibre reinforced concrete (UHPFRC) and carbon fibre reinforced polymer (CFRP) has been done analytically in ABAQUS. The seismic parameters observed are the hysteresis response, strength, stiffness, ductility and energy dissipation of the specimens strengthened both by UHPFRC and CFRP. From the results it is clear that the combination of the two strengthening schemes is very efficient in increasing the peak load 2.62 times and the ductility by almost 6% of the specimens as compared to the specimens strengthened using only one scheme. Also the energy dissipation shows an increase of 7.3% in case of using the combination strengthening strategy. The rate of degradation of the strength is also reduced substantially.

Keywords: Seismic performance, Modelling, ABAQUS, UHPFRC, CFRP, Strengthening

1. Introduction

A beam column joint is subjected to shear, tension and compression due to the various loads acting on the structure. The demand of performance of the beam column joint is higher in case of seismic loading because when an earthquake strikes a building can move in any direction and various stresses are generated due to the push and pull of the bars that results is fatigue and geometric distortion of the joint. Thus, a degradation in strength and stiffness is obvious which makes it the weakest element in the whole structure that could lead to the collapse of the whole structure and render it unsuitable. Additionally, the external beam column joint is the more vulnerable to seismic loading due to the discontinuity of the geometry and it demands to explore the parameter of bond slip of reinforcement [1]. Thus, a beam column joint needs strengthening as it is an economic and immediate remedy rather than replacement. Strengthening of structure is required in the present day and age because of the continuously changing seismic hazard levels, seismic load levels, and design method and serviceability requirements. Also, continuous research is required to find the best, economic, and suitable to any type of condition method of strengthening so that the basic objective of strengthening that are public safety, structure survivability, structure functionality, and structure unaffected are fulfilled.

1.1. Strengthening Techniques

There are various techniques by which strengthening of the members can be done explored in the literature. Tsonos A [2] observed that cast in place concrete jacket is better than shotcrete jacket due to proper confinement provided to the reinforcement. Shaaban et al [3] observed that more the number of layers of reinforcement in ferro-cement, higher is the ductility, strength etc. and also the orientation angles of the wire mesh in the reinforced concrete thin walls of ferro-cement effects the results. Grouting of members for reducing the cracks and voids was done by injecting the slurry under pressure which resulted in the reduction of splitting of concrete in the members once the load is applied [4] [5]. Steel jacketing is done using the adhesively bonded steel plates and steel strips with the result depending on the varying strip spacing and thickness of the bonded plates [6] [7] [8]. The effect of FRPs strengthening on BCJ shows the effect of orientation, grooving/bonding, anchoring, embedded nature, thickness and layers among various other factors on the strength imparted by it in strengthening the members. Ha G et al [9] strengthened specimens using CFRP embedded bars with externally

*Corresponding author. Tel: +917042443214; E-mail address: qurrainfayaz94@gmail.com

Published online: December 19, 2022
doi:10.38208/acp.v1.599

bonded CFRP sheets due to which flexural cracks are minimized because of the better confinement. Esmaeeli E et al [10] [11] observed the difference in parametric results by applying the CFRP on only two sides of some specimens and fully confining the specimens on all the sides where the results indicated that full confinement provides better results. Mahmoud M et al [12] used CFRP near surface mounted strips along with sheets to strengthen the specimens. Orientation of CFRP was the basic criteria largely affecting the results of strength and ductility. Realfonzo R et al [13] highlighted the effect of not mechanically anchoring the CFRP to the specimen which results in quicker delamination of the sheets. Roy B et al [14] strengthened the specimens by GFRP to observe an increase in strength, ductility w.r.t. monolithic control and jointed specimen (construction joint in column) and it was observed that parameters showed a greater increase in case of the jointed specimens. Mostofinejad D et al [15] [16] strengthened the specimens by CFRP by grooving them at the joint region in X-shape and an increase in capacity was observed in all of them thus highlighting the effect of both the bonding technique as well as the orientation although de-bonding was the basic criteria of failure but strength obtained was much higher. X-shaped orientation of the CFRP for strengthening the specimen has been observed to provide full restraint to the joint from all sides so that the fiber utilizes the plastic flow of matrix to transfer the load to the fiber which results in high strength [17]. Dalalbashi A et al [18], Ronagh H et al [19] compared the effect of CFRP and GFRP in lateral load carrying capacity which indicated the improvement in case of using CFRP was twice as that of GFRP. In recent years the advent of Ultra High Performance Fibre Reinforced Concrete has greatly influenced the field of strengthening and retrofitting because of better properties than other schemes. It is evident from the literature the various methods and techniques of strengthening/retrofitting of structure despite having their various advantages, have their share of disadvantages. Few to mention are an increase in cross section and weight due to concrete jacketing which also renders the structure un-alluring. Steel jacketing is subject to degradation due to corrosion. Ferro-cement is also subjected to corrosion due to incomplete cover provided by the mortar. Epoxy injections perform poorly where moisture is present in environment. FRPs have a de-bonding problem in shear deficient beam-column joint as well as anchorage problem. These issues have led the search for a better advanced material like High Performing Fibre Reinforced Concrete along with different cementitious composites which addresses these disadvantages due to its good properties, better bond characteristics and higher energy dissipation capacities. According to literature a concrete with a compressive strength greater than 100 MPa [20] [21] [22] [23] is accepted as the Ultra High Performance Fibre Reinforced Concrete which also has a tensile strength of 7-10 MPa [22] [24] [25] [26] along with a flexural strength of greater than 30 MPa [27]. Richard P, Cheyrezy M [28] have reported that the ductility of UHPFRC is 250 times greater than that of normal concrete. Voort V [29] observed that the low porosity of Ultra High Performance Fibre Reinforced Concrete w.r.t. normal concrete results in increased durability. Study of bond characteristics of Ultra High Performance Fibre Reinforced Concrete and Normal Concrete has been done from the results of slant shear, splitting tensile and direct shear tests which highlight the excellent bond properties of UHPFRC with NC. In all the tests the failure of the weaker concrete occurs rather than the failure of bond [30] [31] [32]. Use of UHPFRC as a strengthening material is being widelly employed now either as a mix used for replacing the normal concrete fully [26] or partially [23] .

1.2. Analytical studies on beam-column joint

Various studies are reported about use of finite element modelling for studying the behavior of strengthened beam column joints including prediction of ultimate loads and cracking patterns. However, the modelling of concrete is the most challenging task. There are various models which simulate the behaviour of concrete. Hsu and Hsu Model 1994 is limited to a concrete of strength 62 MPa, Park and Paulay Model 1975 considers concrete as an elastic–plastic and strain hardening material. These are all suitable in the compression zone but for tension zones the models used are smeared crack model, fictitious crack model, and crack-band theory [33].

Mosallam A et al [34] numerically investigated the behaviour of 5 of the 8 experimentally tested interior RC beam-column joint retrofitted with different types of FRP composite laminates and hybrid connectors subjected to both gravity and low-frequency full-cyclic reversal loads except for one of the control specimen which is subjected to dynamic impulse loading. The modelling is done in the ABAQUS software conventionally for all the elements. Control Specimen (AB-2) and retrofitting with high-strength carbon/epoxy composite laminates (RS-SC), high-modulus carbon/epoxy laminates (RS-MC), E-glass/epoxy external laminates (RS-G) and the light-weight hybrid composite connector for bond-slip retrofit (RS-SCC). The load displacement curves for the experimental and numerical specimens are compared and it is observed that there is a good agreement between the experimental data and FE model specifically in the linear range. RS-SCC, RS-SC, RS-G and RS-M show an increase of 55%, 34.1%, 12.7% and 10.85% in the peak load over AB-2 respectively. Farzad M. et al., 2019 [35] analysed the bond behaviour experimentally as well as numerically between normal concrete as substrate and UHPC as overlay in both wet and dry conditions of the substrate to ascertain the load capacities on the basis of slant shear, direct shear and third point flexural beam test. The model to be tested is based on two concepts, first is the conventional tie model where the nodes in the same plane share displacement and second is the use of an intermediate layer of concrete of 100μm thickness to act as in interface between the substrate and the overlay. The results indicated that the model using material contact showed much accurate results than the model using tie contact by limiting the error to 18% for the contact layer model as compared to 150% for the tie model when subjected to shear and tension combined. However when the tie model is subjected to combined shear and compression the error is limited to 22%.

The basic problem that is observed in any of the strengthening/retrofitting technique is the rate of deterioration of the materials that are used for the purpose of providing an enhanced strength, ductility and energy dissipation. This results in limited use of the capacity of the materials which then results in economic losses also. In CFRP the major problem is of de-bonding which can be overcome by using it alongside UHPFRC in strengthening. It results in

the UHPFRC taking a major part in the energy dissipation thus reducing the negative effects of de-bonding on CFRP and the CFRP in return helps in utilising the maximum potential of the UHPFRC by providing a much better confinement at the later stages of loading and deterioration . So to overcome this particular drawback a combination of two retrofitting strategies is required that together increase the performance of the structure strengthened and complement each other in maintaining the integrity of the strengthening scheme.

Based on the above drawn conclusions the objective set for this study is to model, verify, analyse, and observe the load displacement behaviour, ductility, strength and stiffness degradation and energy dissipation of the specimens strengthend by the scheme discussed above.

2. Verification of the modelling process

Firstly, a model has to be developed to validated the process. This is done using the experimental results from the literature. For this, a set of 3 specimens are selected from Khan M. et al., [22] to establish validation of the model. One was a control specimen (TC) tested at ±4.89% drift ratio and the other two are specimens strengthened by casting UHPFRC jackets around the control specimen after preparing the surface using the sandblasting technique for a good bond.These specimens are then tested at two different drift ratios – TS1 (±8.67%) and TS2 (±4.89%) so that the difference in the load carrying capacity, ductility, energy dissipation can be observed due to the possible detachment of the UHPFRC and NC at higher damage levels or drift ratios. The detailing of all the specimens was same so as to get an absolute idea of the strengthening procedure.

The numerical modelling was carried out using the ABAQUS FE software to study the behavior of the strengthened beam column joints under cyclic loading. It consisted of modelling the geometry of the specimens along with their materials such as concrete, steel and CFRP, the loading and constraints, also the contact/interaction between the materials. The NC, UHPFRC, and steel-plates were modeled using the 3-D eight-noded brick elements. Whereas, the reinforcement steel were modeled with two noded 3D truss elements. In ABAQUS the static general method was used for simulating the FE models.

Table 1 Experimental Specimens to be verified in ABAQUS

Specimen	*Details*
TC	Control Specimen tested under reverse cyclic loading up to a drift of ± 5%
TS1	Strengthened Specimen using the sand blasting technique to create a good bond between the NSC and in-situ casted UHPFRC tested under reverse cyclic loading up to a drift of ± 8.7%
TS2	Strengthened Specimen using the sand blasting technique to create a good bond between the NSC and in-situ casted UHPFRC tested under reverse cyclic loading up to a drift of ± 5%

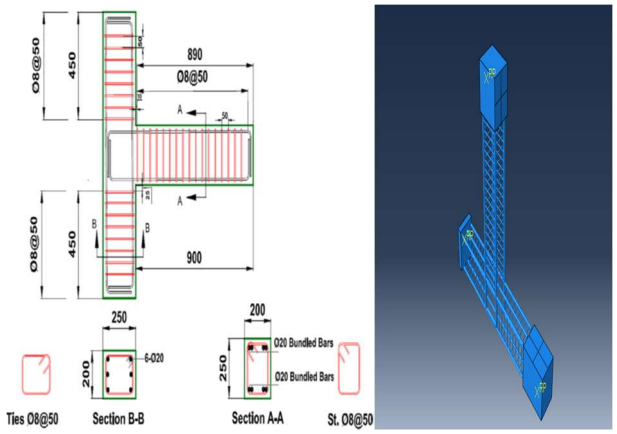

Experimental FE Model

Figure 1 Control Specimen TC

2.1. Material Modelling

2.1.1. Concrete Modelling

For modelling concrete, often the plasticity theory is used. But this theory performs satisfactorily only in the compression zone. For tension zones, various other models such as the smeared crack model, fictitious crack model etc. are utilized. Thus the need to inculcate both the models into a single model resulted in the development of "Concrete Damage Plasticity" model which was developed by [36] that is an adjustment of the Drucker-Prager strength hypothesis and further elaborated by [33]. In this model, basically two modes of failure of concrete are considered. First is the cracking due to tension and second is the crushing due to compression. Apart from the strength parameters, the deterioration parameters are also required for a much accurate behavior. Thus, this model requires the uniaxial stress-strain values for both under compression as well as tension and the concrete damage parameters (dc &dt) under compression and tension using the Birtel and Mark equations [37].

The properties and CDP parameters of concrete used are:

Table 2 Concrete Properties and CDP Parameters

Properties	***Normal Concrete***	***UHPFRC***
E	25.7 GPa	52.4 GPa
μ	0.19	0.2
Average Compressive Strength	30 MPa	145 MPa
Split Tensile Strength	3.1 MPa	8.51 MPa
Specific Weight	2300 kg/m³	2300 kg/m³
CDP Parameters		
Dilation Angle	35°	40°
e	0.1	0.1
fb0/fc0	1.16	1.16
K	.667	.667
Viscosity Parameter	0.007985	0.007985

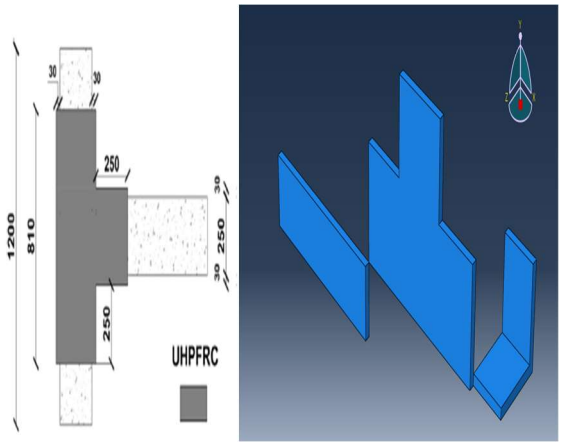

Experimental FE Model

Figure 2 UHPFRC plates in TS1 and TS2

The properties of steel used are:

Table 3 Steel Properties

Properties	***Longitudinal Bars***	***Shear Reinforcement***
E	195.1 GPa	195.1 GPa
μ	0.3	0.3
Yield Strength	605 MPa	605 MPa
Ultimate Tensile Strength	695 MPa	695 MPa
Bar Diameter	20 mm	8 mm
Specific Weight	7800 kg/m³	7800 kg/m³

2.1.2. Steel Modelling

The reinforcement in the ABAQUS FE software can be modelled on the basis of two laws. First being the bi-linear stress strain behavior and second being the multi-linear stress strain behavior. The multi-linear law is assumed because of the availability of the sufficient information of the yield and ultimate stress and strain.

The interaction is set to embedded region for the concrete and reinforcement to simulate a perfect bond with no slip as enough development length is available for the friction in the experimental setup, while a cohesive bond is defined on the concrete surface for attaching CFRP to the surface. Further a tie constraint is defined for the interaction between the rigid loading plate and normal concrete surface. Tie constraint is also used in TS1 and TS2 strengthened specimens to simulate a perfect bond between the UHPFRC and NC as no de-bonding is observed experimentally.

2.2. Loading and Boundary Conditions

The boundary conditions are defined as pinned supports with a constant axial load of 150 kN on the column and loading history as defined the same way as in the experiment at the end of the beam to subject the specimens to cyclic loads.

The hysteresis responses of all the specimens are obtained and the results closely match in terms of initial stiffness, peak load in the positive as well as negative direction except for the pinching effect which could not be

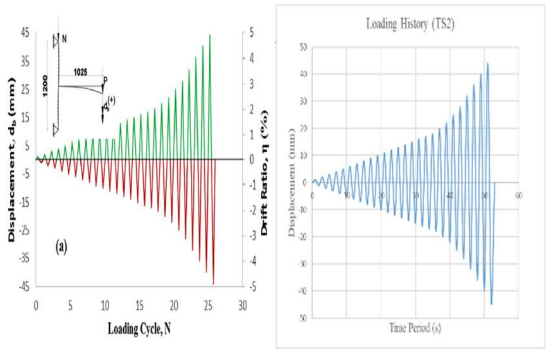

Experimental Analytical

Figure 3 Loading History for TC, TS2

observed due to the limitations of the software. The deviation in the peak load by a factor of 14% - 25 % for TC, TS1 and TS2 is because of the assumption of the tie constraint which simulates a perfect bond. Also the peak load is observed at an earlier displacement. It is due to the higher stiffness of the structure, simulated due to a high dilation angle in the ABAQUS software than in an actual specimen. Assumptions in the material properties due to data insufficiency and the presence of cracks in the actual specimens leads to this overestimation [34].

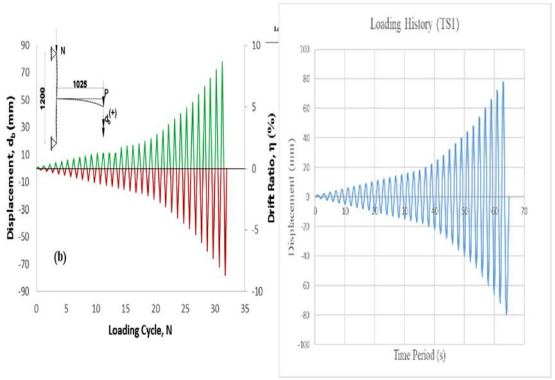

Experimental Analytical

Figure 4 Loading History for TS1

2.3. Validation of Experimental and F.E. results

Obtained numerical results are compared to experimental data reported by [22]. For the specimens the load displacement hysteresis response experimentally and numerically is compared as shown in Figures 5, 6, & 7.

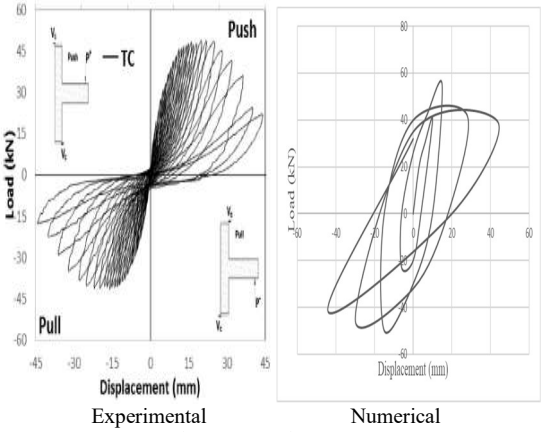

Experimental Numerical

Figure 5 Specimen TC

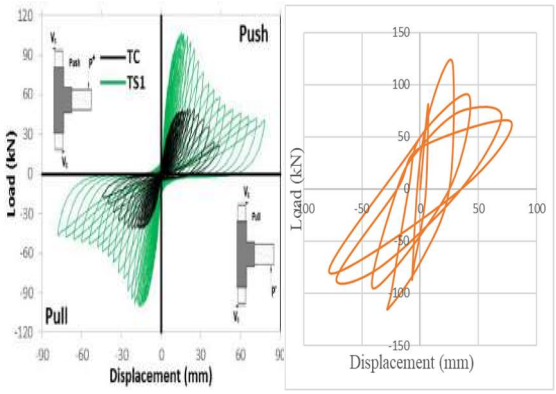

Experimental Numerical

Figure 6 Specimen TS1

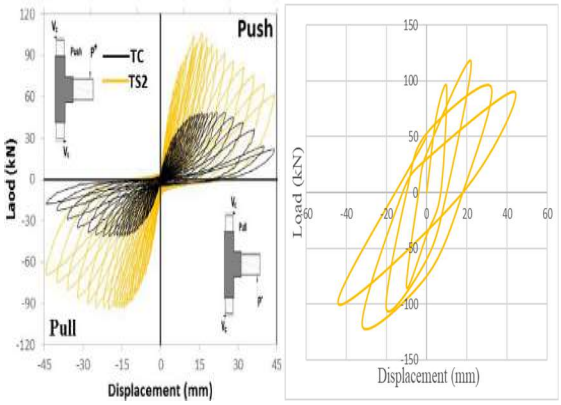

Experimental Numerical

Figure 7 Specimen TS2

The increase in the peak load as observed in the TS1 and TS2 specimens with respect to TC specimen is basically due to the full participation of UHPFRC at earlier drift ratios because of its good bond characteristics with the Normal Concrete substrate of TC specimen when it is strengthened with UHPFRC plates. This behavior is validated from the literature also [35].

The objective of loading the TS1 specimen up to a higher drift ratio than TS2 is to basically analyse the behaviour of the bond between UHPFRC and NC. Experimentally, it detatches in layers after a drift ratio of ±6%. This results in a reduced load after that drift ratio and also in increased rate of strength degradation. Numerically, since it is considered as a perfect bond, the degradation in stifness is slower. Subsequently the load at ultimate displacement is higher.

3. Modelling of specimens strengthened using UHPFRC and CFRP

Based on the validation of the specimens of [22] , a parametric study regarding the specimens strengthened using both the UHPFRC and CFRP is done to predict the behaviour of the exterior beam column joint. The material is modelled the same as in [22] with CFRP properties being taken from [38] and modelled as below:

3.1. CFRP Modelling

For our strengthening scheme, along with UHPFRC unidirectional FRP sheets are used to strengthen the R.C beam-column joint model further. The fibre behaviour is linear elastic up to failure with rupture failure. A lamina linear elastic element is used to model FRP. The mechanical properties for the combined CFRP sheet and adhesion using epoxy are evaluated as proposed by Mallick PK [39]. The parameters required in the ABAQUS for defining the properties of CFRP are the engineering constants given in Table 4.

Table 4 CFRP + Epoxy properties

E1 *(Elastic modulus in the longitudinal direction)*	106,509 MPa
E2 *(Elastic modulus in the transverse direction)*	33,970 MPa
υ *(Poisson's ratio)*	.31
G11 *(Plane shear modulus)*	12400 MPa
G12 *(Plane shear modulus)*	12400 MPa
G13 *(Normal to the plane shear modulus)*	13,065 MPa

The specimens investigated are:

Table 5 Specimen strengthened using UHPFRC and CFRP

Specimen	Details
TC-C	Control Specimen strengthened with CFRP tested under reverse cyclic loading up to a drift of ± 5%
TS1-C	Strengthened Specimen using the sand blasting technique to create a good bond between the NSC and in-situ casted UHPFRC and CFRP tested under reverse cyclic loading up to a drift of ± 8.7%
TS2-C	Strengthened Specimen using the sand blasting technique to create a good bond between the NSC and in-situ casted UHPFRC and CFRP tested under reverse cyclic loading up to a drift of ± 5%

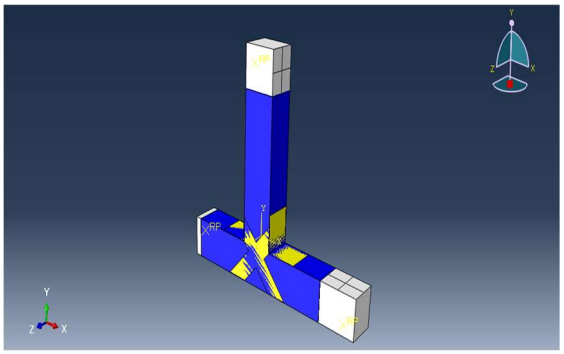

Figure 8 Geometrical Model of TC-C

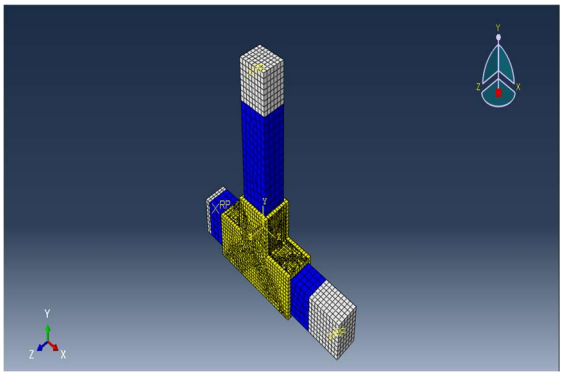

Figure 9 Geometrical of model of specimens TS1-C and TS2-C

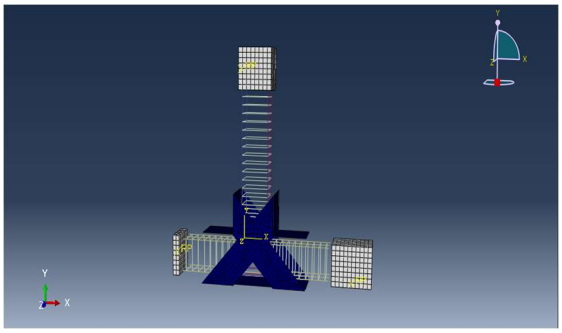

Figure 10 CFRP around the joint region

The CFRP is defined as a deformable shell in ABAQUS. The orientation of the CFRP for strengthening the specimen is chosen so as to provide full restraint to the joint from all sides so that the fiber utilizes the plastic flow of matrix to transfer the load to the fiber which results in high strength [17].

4. Results

4.1. Load Displacement Hysteresis Curves of TC-C, TS1-C, TS2-C.

All the strengthened specimens are tested under the cyclic load up to their respective displacements. The control specimen strengthened with CFRP only (TC-C), shows a peak load of 70.1 kN at a displacement of about 15 mm in the positive direction and a peak load of 78.9 kN at a displacement of about 17 mm in the negative direction. This when compared with the numerically modelled control specimen (TC) shows an increase of an average of 25 % in the peak load capacity.

The second specimen strengthened with both UHPFRC and CFRP (TS1-C), shows a peak load of 144.73 kN at a displacement of 26 mm in the positive direction and a peak load of 137 kN at a displacement of 28 mm. Comparing it to the numerically modelled specimen strengthened by only UHPFRC (TS1) shows an average increase of 17 %.

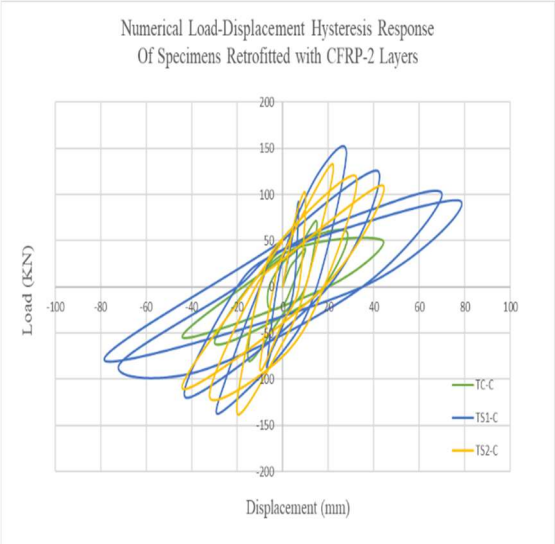

Figure 11 Numerical Hysteresis Response of TC-C, TS1-C, and TS2-C

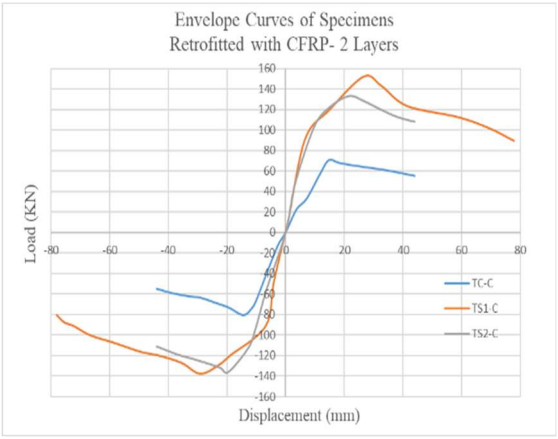

Figure 12 S-Curves of Specimens Strengthened with CFRP- 2 Layers

The third specimen strengthened with both UHPFRC and CFRP (TS2-C), shows a peak load of 132.8 kN at a displacement of 21 mm in the positive direction and a peak load of 137 kN at a displacement of 20 mm which when compared to the numerical model of the specimen strengthened by only UHPFRC (TS2) shows an increase of 14% on average.

4.2. Envelope Curves of TC-C, TS1-C, TS2-C.

It can be clearly seen in Figure 12 that the initial stiffness of all the specimens modelled in ABAQUS is higher which results in a higher peak load than what could be anticipated in the experimental setup. This increase in strength is due to the absence of micro-cracks present in the software modelled specimens which otherwise occur in real situations and the higher dilation angle value of the UHPFRC material.

Comparing the values of the peak load, the TS1-C specimen has the highest by an average of 4.4% and 60% with respect to TS2-C and TC-C.

4.3. Ductility of TC-C, TS1-C, TS2-C.

Ductility describes the extent to which a structure can undergo large deformations without failing. It is used to designate the amount of large lateral displacements that can be imposed on the specimens by loading it in a cyclic manner. The ductility of the specimens numerically tested is calculated from their respective envelope curves [23].
Pu is the peak load observed in the cycle.

Yield Stress is taken as 0.8×Pu and the displacement at this stress level is taken as the Yield Displacement.

Hence, the calculated values are:

Table 6 Calculation of Ductility

Specimen	***TC-C***	***TS1-C***	***TS2-C***
Pu (positive)	70 kN	145 kN	133 kN
0.8 Pu	56 kN	116 kN	106 kN
Pu (negative)	80 kN	137 kN	137 kN
0.8 Pu	64 kN	110 kN	110 kN
δy1	12 mm	13 mm	10 mm
δy2	10 mm	15 mm	12 mm
δu1	43 mm	50 mm	44 mm
δu2	28 mm	53 mm	44 mm
$\mu=\frac{\delta_{u1}+\delta_{u2}}{\delta_{y1}+\delta_{y2}}$	**3.23**	**3.68**	**4**

The ductility values clearly indicate the efficiency of the usage of UHPFRC and CFRP together as a confining material with an increase of 14% for TS1-C and 23.8% for TSC-2 over control specimen retrofitted with just CFRP (TC-C). The values TC-C, TS1-C, and TS2-C when compared to the ductility values of numerically verified specimens TC, TS1, and TS2 show an increase of 12.1 %, 1.1 % and 5.2 % respectively highlighting the effect CFRP has in combination with UHPFRC.

4.4. Strength and Stiffness Degradation of TC-C, TS1-C, TS2-C.

As seen in Figure 13 the reduction in strength for all the specimens is more in the negative displacement which confirms the weak behavior of concrete in tension. But comparing TC-C, TS1-C and TS2-C at the same displacement the reduction in strength is more in the TC-C specimen due to the absence of UHPFRC which has a much higher tensile strength when compared with normal concrete and also provides a much better confining action than CFRP which is susceptible to de-bonding.

The peak to peak stiffness of control and retrofitted initially damage specimen tested under quasi-static reverse cyclic loading is calculated for each drift ratio. The slope of the line joining the peak point reached on positive and negative directions in a loading cycle is defined as peak to peak stiffness. [40].

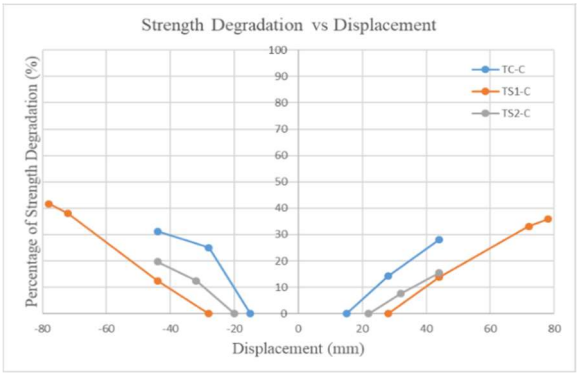

Figure 13 Degradation of Strength vs Displacement

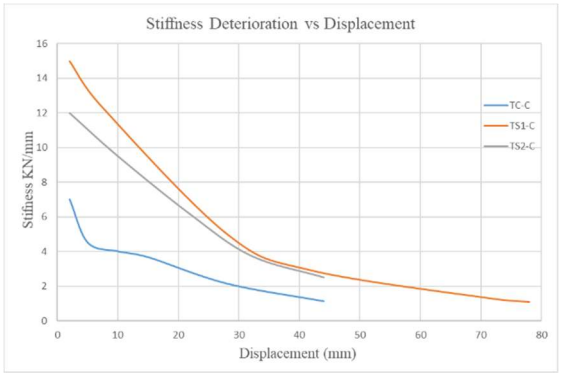

Figure 14 Reduction in Stiffness vs Displacement

It can be seen in Figure 14 that there is an abrupt loss of stiffness in the control specimen strengthened only by CFRP at a lower displacement level as compared to the specimens strengthened by both UHPFRC and CFRP. This is due to the absence of the extra confining action of the UHPFRC. TS1-C and TS2-C even when subjected to further displacements, the stiffness remains well above the TC-C due to the kicking in of the CFRP action to maintain the required stiffness.

4.5. Energy Dissipation of TC-C, TS1-C, TS2-C.

The energy dissipated by the specimens is calculated by the area enclosed in the hysteresis loop of a drift ratio. A loop is said to be closed when a cycle is completed, i.e., positive and negative displacement both occurs. This subjects a point in a joint to both compression and tension in once complete cycle.

As can be seen in Figure 15 the highest energy is dissipated by the TS1-C specimen at each drift ratio. The energy dissipation of the specimen TS2-C is less in the last few cycles due to it reaching the peak load at an earlier drift ratio which lead to its early damage.

The TS1-C and TS2-C dissipate a cumulative energy of 1.55 and 1.22 times higher that of TC-C at the same drift ratio of ±4.89%. This shows the better effect of using UHPFRC with CFRP.

The energy dissipated by TC-C, TS1-C, and TS2-C specimens is higher than TC, TS1, and TS2 specimens by 12.9%, 1.4 % and 6.9% respectively at ±4.89 % drift ratio highlighting the use of CFRP alone and in combination with UHPFRC.

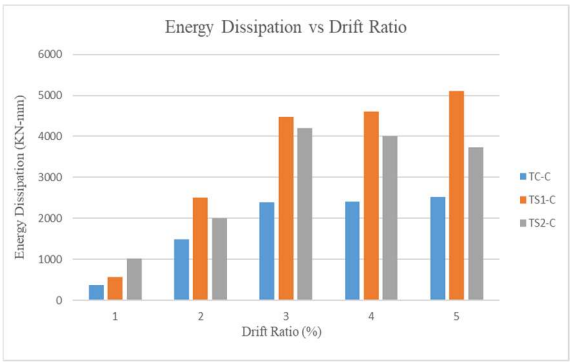

Figure 15 Energy Dissipation per Drift Ratio

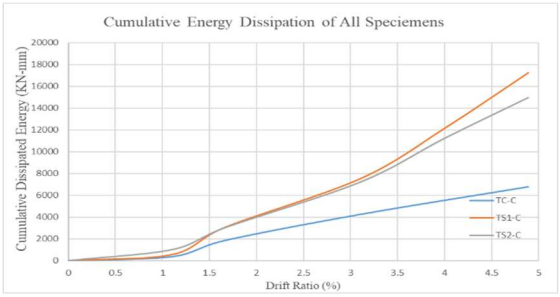

Figure 16 Cumulative Energy Dissipation

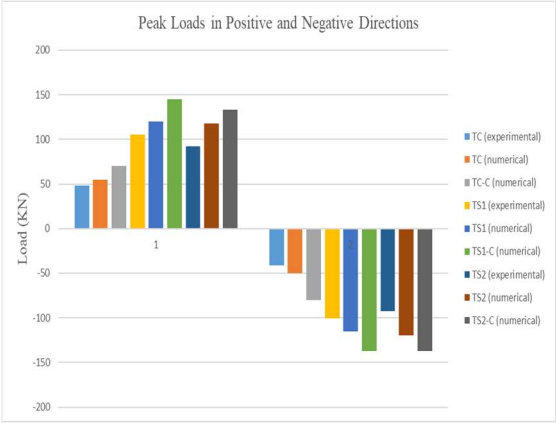

Figure 17 Comparison of Peak Loads Experimentally and Numerically with and without CFRP

4.6. Comparison of Peak Loads

For control specimen (TC) and control specimen strengthened by CFRP (TC-C) tested at same drift ratio of ±4.89% gives an increase in peak load by about 30 % for TC-C specimen indicating the action of CFRP in strengthening the joint.

For specimens tested at same drift ratio of ±8.69% and strengthened by both UHPFRC and CFRP an increase in peak load by about 19 % for TS1-C specimen is observed which otherwise without CFRP would detach from the Normal Concrete.

For TS2 and TS2-C specimens tested at same drift ratio of ±4.89% gives an increase in peak load by about 13% for TS2-C specimen. Numerically modelled TS1-C and TS2-C specimens shows an increase of 2.62 times when compared to numerically modelled TC specimen. This increase in strength is attributed to the contribution of CFRP in providing an assistance to the UHPFRC to take more load without rapid disintegration.

5. Conclusions

1. The numerical model developed for the experimental program by [22] is validated within reasonable limits. A deviation of 14-20% is observed in the value of peak load for all the modelled specimens namely TC, TS1, and TS2 from the experimental results because of the assumption of the tie constraint which simulates a perfect bond and the absence of micro cracks that aren't present in the software modelled specimens.
2. For the UHPFRC and CFRP strengthened BCJ specimens TC-C, TS1-C and TS2-C the increase in strength is by a factor of 2.7, 2.1 and 1.3 times than that of TC, TS1 and TS2 (analytical) respectively.
3. The ductility values clearly indicate the efficiency of the usage of UHPFRC and CFRP together as a confining material with an increase of 14% for TS1-C and 23.8% for TSC-2 over control specimen retrofitted with just CFRP (TC-C). Specimens strengthened using the combination of CFRP and UHPFRC (TC-C, TS1-C, TS2-C) show an increased ductility of about 6 % than the specimens strengthened using only one scheme (TC, TS1, TS2-analytical).
4. The degradation in the strength at ±4.89% drift ratio was observed to be 30%, 19% and 14% for specimens TC-C, TS1-C, TS2-C. Moreover for specimen TS1-C the degradation in stiffness was observed to be 40% at an ultimate drift ratio of ±8.67%. Thus a combination of UHPFRC and CFRP drastically reduces the strength degradation.
5. The initial stiffness of the specimens retrofitted with CFRP and UHPFRC, TS1-C and TS2-C is higher than TC-C by 4.0 and 3.4 times which is partly due to the higher dilation angle of the UHPFRC and mostly because of combination of UHPFRC and CFRP.
6. The TC-C specimen dissipates an energy of 6775 KN-mm which is 13 % more than TC (analytical) specimen at the ultimate drift ratio of ±4.89%. Specimen TS1-C dissipates an energy equal to 17240.5 KN-mm at the same drift ratio of ±4.89% which is 1.4% more than TS1 (analytical). The energy dissipated by specimen TS2-C is of value of 14973 KN-mm which is 6.9% more than TS2 (analytical) at its ultimate drift ratio of ±4.89%. This increase in energy dissipation is attributed mainly to the presence of UHPFRC as a strengthening material and also the CFRP which helps in maximizing the potential of UHPFRC by providing a confining action to the concrete.

Disclosures

Free Access to this article is sponsored by SARL ALPHA CRISTO INDUSTRIAL.

References

1. Pampanin S, Christopoulos C. Non-invasive retrofit of existing RC frames designed for gravity loads only. In: Fib symposium on concrete structure in seismic regions, Athens, 2003.
2. Tsonos A. Performance enhancement of R/C building columns andbeam-column joints through shotcrete jacketing. Engineering Structures, 2010; 32(3), 726-740.
3. Shaaban I, Seoud O. Experimental behavior of full-scale exterior beam-column space joints retrofitted by ferrocement layers under cyclic loading. Case Studies in Construction Materials, 2018; 8, 61-78.
4. Karayannis CG, Sirkelis GM. Strengthening and rehabilitation of RC beam–column joints using carbon-FRP jacketing and epoxy resin injection, 2008.
5. Zhang Y, Jiangtao Y, Zhoudao L, Lei T, Hui S. Seismic Performance of RC frame Retrofitted by Epoxy Injection Technique Tested on Shaking Table. Research Institute of Structural Engineering and Disaster Reduction, Tongji University, Shanghai, China, 2012.

6. Yang Y, Xue Y, Wang N & Yu Y. Experimental and numerical study on seismic performance of deficient interior RC joints retrofitted with prestressed high-strength steel strips. Engineering Structures, 2019; 190, 306-318.
7. Yen J, Chien H. Steel plates rehabilitated RC beam-column joints subjected to vertical cyclic loads. Construction and Building Materials, 2010; 24(3), 332-339.
8. Campione G, Cavaleri L, & Papia M. Flexural response of external R.C. beam-column joints externally strengthened with steel cages. Engineering Structures, 2015; 104, 51-64.
9. Ha G, Cho C, Kang H, & Feo L. Seismic improvement of RC beam-column joints using hexagonal CFRP bars combined with CFRP sheets. Composite Structures, 2013; 95, 464-470.
10. Esmaeeli E, Joaquim AOB., Fasan JSCL, Prizzi FRL, Melo J & Varum H. Retrofitting of interior RC beam–column joints using CFRP strengthened SHCC: Cast-in-place solution. Composite Structures, 2014; 122, 456–467.
11. Esmaeeli, E, Danesh F, Tee K, & Eshghi S. A combination of GFRP sheets and steel cage for seismic strengthening of shear-deficient corner RC beam-column joints. Composite Structures, 2017; 159, 206-219.
12. Mahmoud M, Afefy H, Kassem N, & Fawzy T. Strengthening of defected beam-column joints using CFRP. Journal of Advanced Research, 2014; 5(1), 67-77.
13. Realfonzo R, Napoli A & Pinilla JGR. Cyclic behavior of RC beam-column joints strengthened with FRP systems. Construction and Building Materials, 2014; 54, 282–297.
14. Roy B, Laskar A. Cyclic Performance of Beam-Column Subassemblies with Construction Joint in Column Retrofitted with GFRP. Structures, 2018; 14, 290-300.
15. Mostofinejad D, Hajrasouliha M. 3D beam–column corner joints retrofitted with X-shaped FRP sheets attached via the EBROG technique. Engineering Structures, 2019; 183, 987-998.
16. Mostofinejad D, Ilia E. Seismic retrofit of reinforced concrete strong beam–weak column joints using EBROG method combined with CFRP anchorage system. Engineering Structures, 2019; 194, 300–319.
17. Singh V, Bansal P, Kumar M & Kaushik S. Experimental studies on strength and ductility of CFRP jacketed reinforced concrete beam-column joints. Construction and Building Materials, 2014; 55, 194-201.
18. Dalalbashi A, Eslami A, & Ronagh H. Plastic hinge relocation in RC joints as an alternative method of retrofitting using FRP. Composite Structures, 2012; 94(8), 2433-2439.
19. Ronagh H, Eslami A. Flexural retrofitting of RC buildings using GFRP/CFRP - A comparative study. Composites Part B: Engineering, 2013; 46, 188-196.
20. Voo YL and Foster SJ. Characteristics of ultra-high performance ductile concrete and its impact on sustainable construction. The IES Journal Part A: Civil and Strutural Engineering, 2010; Vol.3, No.3, pp. 168-187.
21. Liang X, Wang Y, Tao Y & Deng M. Seismic performance of fiber-reinforced concrete interior beam-column joints. Engineering Structures, 2016; 26 (2016) 432–445.
22. Khan M, Al-Osta M, Ahmad S, & Rahman M. Seismic behaviour of beam-column joints strengthened with ultra-high performance fibre reinforced concrete. Composite Structures, 2018; 200, 103-119
23. Sharma R, Bansal P. Behaviour of RC exterior beam column joint retrofitted using UHP-HFRC. Construction and Building Materials, 2019; 195, 376-389.
24. Habel K, Denarie E, & Bruhwiler E. Experimental Investigation of Composite Ultra-High-Performance Fibre-Reinforced Concrete and Conventional Members. ACI Structural Journal, 2004; Vol.104, No.1.
25. Voo YL, Augustin PC, & Thamboe TAJ. Construction and Design of a 50M Single Span UHP Ductile Concrete Composite Road Bridge. The Structural Engineer, the Institution of Structural Engineers, UK, 2011; Vol.89, No.15, pp.24-31.
26. Saghafi M, Shariatmadar H. Enhancement of seismic performance of beam-column joint connections using high performance fibre reinforced cementitious composites. Construction and Building Materials, 2018; 180, 665-680.
27. Wuest J. Structural behaviour of reinforced concrete elements improved by layers of ultra-high performance reinforced concrete, 2006; 6th International PhD Symposium in Civil Engineering Zurich.
28. Richard P, Cheyrezy M. Composition of reactive powder concretes. Cement and concrete research, 1995; Vol. 25, No.7.pp.1501-1511.
29. Voort V. Design and field testing of tapered H-shaped Ultra High Performance Concrete piles, Iowa State University, 2008.
30. Tayeh B, AbuBakar B, Johari MM & Voo Y. Utilization of ultra-high performance fibre concrete (UHPFC) for rehabilitation a review. Procedia Engineering, 2013; 54, pp. 525-538. Elsevier Ltd.
31. Carbonell MMA., Harris DK, Ahlborn TM, Froster DC. Bond performance between ultrahigh-performance concrete and normal-strength concrete. J Mater Civ Eng Aug. 2014; 26 (8):04014031.
32. Zhang Y, Liao PZZ & Wang L. Interfacial bond properties between normal strength concrete substrate and ultra-high performance concrete as a repair material. Construction and Building Materials, 2019; 235.
33. Lee J, Fenves G. Plastic-damage model for cyclic loading of concrete structures. J Eng Mech, 1998; 124(8):892–900.
34. Mosallama A, Allam K & Salama M. Analytical and numerical modeling of RC beam-column joints retrofitted with FRP laminates and hybrid composite connectors. Composite Structures 214, 2019; 486–503.
35. Farzad M, Shafieifar M & Azizinamini A. Experimental and numerical study on bond strength between conventional concrete and Ultra High-Performance Concrete (UHPC). Engineering Structures 186, 2019; 297–305.
36. Lubliner J, Oliver J, Oller S & Oñate E. A plastic-damage model for concrete. International Journal of Solids Structure, 1989; 25(3):299–326.

37. Birtel V, Mark P. Parameterized finite element modelling of RC beam shear failure. ABAQUS users' conference, 2006; pp 95–108.

38. Abu-Tahnat YB. Effect of using fiber reinforced polymers on the ductility of retrofitted reinforced concrete joint. [MSc. Thesis]. Nablus, Palestine: An-Najah National University; 2018.

39. Mallick PK. Fiber-reinforced composites. New York: Marcel Dekker, 1993.

40. Antonopoulos CP, Triantafillou TC & Asce M. Experimental investigation of FRP-strengthened RC beam-columnjoints. J. Compos. Constr. 7, 2003; 39–49.

41. Simulia D S. ABAQUS 6.13-4 User's manual. Dassault Systems, Providence, RI. 2013.